

Electrochromic Polymer Ink Derived from a Sidechain-Modified EDOT for Electrochromic Devices with Colorless Bright State

Sven Macher,^[a] Mauro Sassi,^[b] Luca Beverina,^[b] Uwe Posset,^[a] Marco Schott,^{*,[a]} Guinevere A. Giffin,^[a] and Peer Löbmann^[a]

Printable organic electrochromic materials are the key component of flexible low power and low weight displays and dynamic shading systems. A vast number of more or less well-performing materials is reported in the literature, but only a very limited number of them have been tested in an industrially-relevant environment so far. Upscaling requires simplicity of synthesis, overall sustainability, low cost and compatibility with simple and high throughput wet-chemical deposition techniques, such as slot-die coating or inkjet printing. In the present paper, an original process is described

that enables the controlled oxidative polymerization of a water insoluble, functionalized 3,4-ethylene dioxythiophene (EDOT) derivative. This process leads to the formation of an ink that consists solely of active polymeric material (no dispersing agents) and has suitable rheological properties for use in roll-to-roll slot-die coating or ink-jet printing. The straightforward deposition, followed by a simple thermal treatment, directly yields stable and homogeneous thin films with state-of-the-art electrochromic performance.

1. Introduction

Flexible electrochromic devices (ECDs) based on transparent, conductive plastic substrates are used as low weight and low power dynamic shading systems and as non-light emitting, flexible display solution. Thus, ECDs have potential applications in the fields of energy-efficient architecture and vehicle glazing as well as in smart consumer goods and environments.^[1]

Organic electrochromic (EC) materials exhibit a reversible and progressive change of their optical absorption that is associated with a redox process. If the material in its pristine form absorbs in the visible region of the electromagnetic spectrum, oxidation or reduction due to an external voltage or current is connected with either a color change or a decoloration. A color change is achieved if both limiting states have absorption in the visible region. Decoloration, on the other hand, is achieved if one of the limiting states has an absorption in the UV or NIR range.^[2]

Conjugated electrochromic polymers (ECPs), such as poly(3,4-ethylene dioxythiophene) (PEDOT) and its derivatives are


one of the main classes of materials exhibiting EC properties as thin films.^[3,4,5] The introduction of solubilizing chains with tailored steric properties, electron donating or withdrawing substituents and copolymerization with intrinsically electron poor units allow a wide range of vivid colors, the possibility of either a color change (e.g. blue to red^[6]) or a decoloration (e.g. blue to colorless^[7]), response times in the range of seconds and high coloration efficiencies.^[8,9–13] While moving from the laboratory to the production-scale, suitable EC performance has to be matched with simplicity of synthetic access, compatibility with high-throughput deposition techniques, straightforward integration into devices and sustainability of the overall process. A vast number of more or less well-performing ECPs is reported in the literature, but only a small selection of them have been tested successfully in an industrially-relevant environment.^[14]


To date, poly(3,4-propylene dioxythiophene) (ProDOT) derivatives are among the best ECPs in terms of synthetic simplicity, optical contrast, coloration efficiency and compatibility with high throughput and large-area deposition.^[11,15,16–18] Although remarkable, ProDOT derivatives still fall short of expectations when employed in dynamic shading systems, one of the most demanding area of application of ECDs, as they do not combine the required optical contrast with a completely colorless bright state.^[12,19] Their residual coloration in the bright state is acceptable in the case of very thin films, but this comes at the expense of sufficient darkening in the colored state.^[20]

Recently, a state of the art polymer based on a PEDOT backbone was introduced, featuring a particularly high optical contrast and a low visible absorption in the bright state (Figure S1). This is the result of the introduction of a terminal double bond at the end of a lateral hexyl side chain (PEDOT-EthC6). Such a functionality is believed to promote a more pronounced π -stacking between neighboring conjugated poly-

[a] S. Macher, Dr. U. Posset, Dr. M. Schott, Dr. G. A. Giffin, Prof. Dr. P. Löbmann
Fraunhofer Institute for Silicate Research ISC
Neunerplatz 2, D-97082 Würzburg, Germany
E-mail: marco.schott@isc.fraunhofer.de

[b] Dr. M. Sassi, Prof. Dr. L. Beverina
Department of Materials Science
University of Milano-Bicocca
Via R. Cozzi 55, I-20125 Milano, Italy

 Supporting information for this article is available on the WWW under <https://doi.org/10.1002/celc.202001595>

 © 2021 The Authors. ChemElectroChem published by Wiley-VCH GmbH. This is an open access article under the terms of the Creative Commons Attribution License, which permits use, distribution and reproduction in any medium, provided the original work is properly cited.

mer chains in the oxidized form, resulting in a complete localization of the polaronic and bipolaronic absorption in the NIR region.^[7,20,21]

Table 1 compares the EC performance of a series of notable ProDOT and PEDOT derivatives, including the terminal double bond bearing PEDOT-EthC6.^[7] A fair comparison between the best ProDOT derivative and PEDOT-EthC6 also has to take into account large-scale processing with industrial relevant roll-to-roll (R2R) coating and printing machines. Although suitably functionalized ProDOT derivatives can be formulated into ready-to-use inks, these processable formulations can only be prepared using Pd-catalyzed coupling reactions and are based on toxic or chlorinated solvents.^[9,11,17,18] Also the solubility of PEDOT-EthC6 in both limiting states is negligible. Nonetheless, PEDOT-EthC6 can be deposited in thin film form by means of *in-situ* polymerization, a reactive ink approach requiring the deposition of a mixture of the EDOT-EthC6 monomer and an oxidizer under carefully controlled conditions. The polymer is obtained directly on the substrate via a thermal treatment, followed by an elaborate rinsing step to remove the oxidizer spent. The process is scalable and affords high quality thin films in an industrially-relevant environment. Although the *in-situ* polymerized PEDOT-EthC6 material shows very promising optical properties, the *in-situ* polymerization process is sensitive to changes in ambient conditions and is time-consuming, mainly because of the need to rinse the polymer thin films in an additional R2R processing step. Thereby, large amounts of solvent waste incur, which has a sizeable ecological impact. Consequently, this deposition method is limited in terms of its cost-saving potential and application flexibility when compared to high-resolution inkjet or screen-printing processes.^[7]

The trade-off between performance and processability is almost as old as the field of ECPs itself. Actually, PEDOT - by far the technically most successful ECP - is completely insoluble in almost all common solvents and only commercially available as the waterborne suspension formulation known under its former trade name BAYTRON P (Bayer AG) and its current trade name Clevios™ (Heraeus Epurio). Such an ink is obtained from the so-called BAYTRON P synthesis, developed at Bayer AG.^[22–24] The water-soluble EDOT monomer is polymerized in an aqueous solution in the presence of a polyelectrolyte (most commonly

polystyrene sulfonate (PSS)), which functions as a counter ion and dispersing agent.^[22–24] The resulting dark blue, aqueous PEDOT:PSS micro-dispersion provides highly conductive and transparent as well as mechanically and environmentally stable thin films.^[3,22,25] Unfortunately, the resulting EC thin film features are well below the standards required for shading applications. Further drawbacks arise from wettability issues, residual water content and – most importantly in the present context – from the fact that this process cannot be applied to water-insoluble monomers, i.e. sidechain-modified EDOT derivatives (e.g. EDOT-EthC6), which offer the possibility to alter the optoelectronic properties of the resulting polymer.^[22–24]

In the present paper, an alternative preparation method is shown that enables the controlled oxidative polymerization of a water insoluble, functionalized EDOT derivative (EDOT-EthC6). This process leads to the formation of a nanoscale, dispersing agent-free ink having suitable rheological properties for the use in R2R slot-die coating or ink-jet printing. The water-free deposition, followed by a simple thermal treatment, directly affords stable and homogeneous thin films with state of the art EC performance. Unlike the previously described *in-situ* polymerization process, this new approach does not require elaborate rinsing of the thermally annealed thin films, as the oxidizing agent is removed during the formulation of the ink. Therefore, it has negligible sensitivity to environmental variables such as temperature and humidity during the deposition process. The control over these variables is de-facto moved from the R2R line to the batch reactor. An additional critical benefit is that the ink is exclusively based on alcohols having negligible toxicity.

The alternative approach is demonstrated with the side-chain-modified EDOT-EthC6 derivative. The polymerization and ink preparation is accompanied by electrochemical analysis of these processes. Thin films of PEDOT-EthC6 are investigated in detail by electrochemical and *in-situ* spectroelectrochemical characterization. The advantages of the presented approach for large-scale production are extremely relevant.

Table 1. Comparison of the EC properties of modified ECPs, in particular modified PEDOT and ProDOT derivatives, with those of non-modified PEDOT and ProDOT.

Polymer	Max. absorption wavelength [nm]	Transmission change [%]	Contrast ratio	Coloration efficiency [cm ² C ⁻¹]	Ref.
PEDOT ^[a]	585	54 (24.8↔78.5)	3.2	137	[16]
PEDOT-EthC6sat ^[b]	564	51 (18.9↔69.9)	3.7	–	[7,13]
PEDOT-EthC6 ^[c]	630	57 (0.8↔57.5)	71.9	530	[7,13]
ProDOT ^[d]	578	66 (13.4↔79.2)	5.9	205	[16]
ProDOT-Me ₂ ^[e]	585	76 (13.1↔89.1)	6.8	277	[16,17]

[a] Poly(3,4-ethylene dioxythiophene). [b] Poly(3,4-(1-hexyloxy)methyl)ethylene dioxythiophene. [c] Poly(3,4-(1-(6-hexenyloxy)methyl)ethylene dioxythiophene. [d] Poly(3,4-propylene dioxythiophene). [e] Poly(3,4-(2-dimethyl)propylene dioxythiophene.

2. Results and Discussion

2.1. Preparation of the PEDOT-EthC6 Ink

The nanoscale ECP ink can be formed from the EDOT-EthC6 derivative, containing a hexenyl sidechain with a terminal double bond. Through the inclusion of a lateral sidechain, the planarity of the conjugated system is improved. Furthermore, intramolecular interactions and high supramolecular order are favored. The consequent narrowing of the band gap results in a bathochromic shift of the polaronic and bipolaronic absorption bands.^[7] As reported in Scheme 1, EDOT-EthC6 is prepared via a Williamson etherification of EDOT-MeOH in anhydrous acetonitrile (ACN) with 6-bromo-1-hexene as the alkylating agent in the presence of sodium hydride (NaH) as the base. The monomer is then oxidatively polymerized in an ACN/H₂O mixture with iron (III)-tosylate as the oxidizing agent in a double-walled reaction vessel (3 h at -8°C).

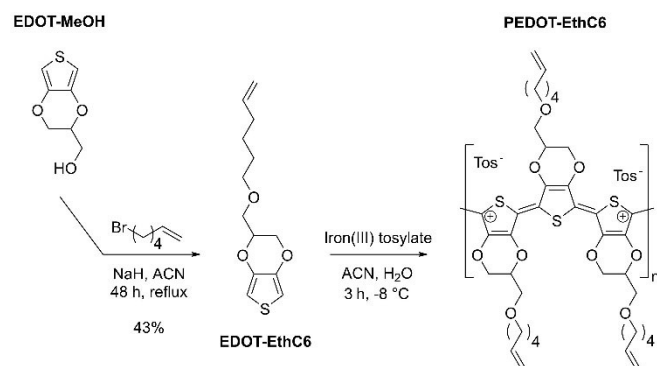
The oxidative polymerization of EDOT and its derivatives in solution is a complex system with numerous influencing factors and intrinsic interactions e.g. between the electron-rich thiophene groups of EDOT-EthC6 and the electron-poor oxidized oligomers, which are easy to oxidize due to their

extended chain length. Furthermore, interactions between the aprotic-polar acetonitrile and the radical cations of the monomers, the oxidized oligomers or the oxidizing agent are possible. In order to gain knowledge of these factors, a detailed analysis of the polymerization was performed by *in-situ* redox potential measurements and GC/MS analysis (Figure 1). The redox potential measurement allows the consumption of the oxidizing agent during the polymerization to be followed. The GC/MS measurements provide information about the monomer concentration in the reaction mixture.

While the monomers and oligomers are oxidized by iron(III) tosylate, Fe^{3+} is reduced to Fe^{2+} . The reduction is associated with a voltage drop, which can be measured in a 3-electrode setup. In the present case, the potential between a platinum electrode and a saturated calomel electrode (SCE) as reference was measured. The redox potential measurement in Figure 1A shows a significant drop after about 48 h. A second drop is observed after 66 h. The curve drops then most sharply at approx. 84 h and levels off again after 96 h. Within 100 h, the potential drops to 0.34 V vs. SCE.

Figure 1B depicts the results of the GC/MS data. The reference compound tetrahydronaphthalene, which is unreactive under the given conditions, is added to the reaction mixture and can be easily identified in the GC/MS data. Samples of the reaction mixture were taken and analyzed by GC/MS. The ratio of the EDOT monomer and the reference allows the monomer consumption to be tracked. The reference compound is only intended to be an internal standard and was therefore added at a much lower concentration than the monomer. Therefore, the mass ratio differs from 1 at the beginning. The GC/MS data shows a substantial decrease of the EDOT/reference ratio, i.e. a significant consumption of monomer, which is almost completed after approx. 70 h.

The monomer is consumed earlier than the oxidizing agent. This can be explained by an oxidation of the oligomers. The oxidation potential of the oligomers decreases with increasing chain length, so that the oxidizing agent consumption is increased by the oxidation of the oligomers and is preferred in



Scheme 1. Synthesis of the EDOT-EthC6 monomer followed by oxidative polymerization in solution at -8°C to obtain the PEDOT-EthC6 polymer.

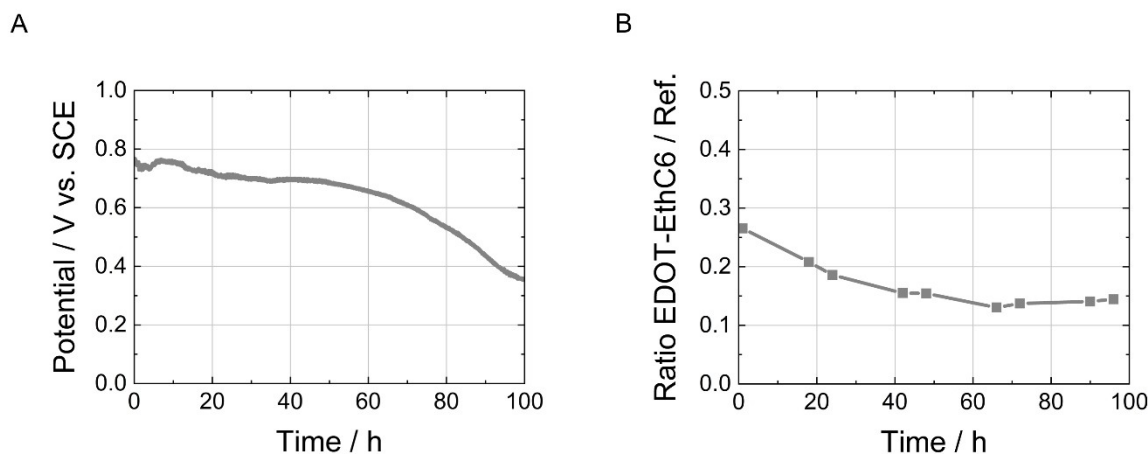


Figure 1. *In-situ* redox potential measurements of the reaction mixture (A) and GC/MS data illustrating the monomer consumption based on decreasing monomer/reference compound ratio (B) during polymerization of EDOT-EthC6 over the course of 100 h.

comparison to the oxidation of monomers. This can also be observed from the redox potential, which decreases progressively with increasing polymerization time. The fact that some monomer remains in the reaction mixture even after 100 h can be explained by the under-stoichiometric oxidizing agent concentration.^[22]

As the oligomer and polymer chains grow during the oxidative polymerization, the different diffusivity of the polymer chains of different molecular weight influences the kinetics of nucleation, so that individual polymer chains of a certain chain length and weight agglomerate in the colloidal environment of the reaction mixture to form nanoparticles. Large polymer agglomerates result in precipitation of the polymer. The precipitate is filtered off prior to coating. Therefore, the particle size distribution is shifted to smaller values. This precipitation leads to a loss of EC performance as the long chain polymers are either filtered off or arrange themselves into inactive macroscopic material clusters on the film. The conductivity of the polymer is not sufficient enough to switch large particle clusters. Smaller particles that do not remain in the filter (e.g. 5 μm pore size) stay in the coating ink and either cause macroscopic clusters on the film or significant light scattering (haze). Agglomerates are difficult to re-disperse. Various re-dispersion methods (intense stirring, ultra sound or shear treatment) can only partially dissolve the agglomerates. As such, there is polymer chain length that depends on the reaction time and represents a trade-off between film quality and EC performance.

The optimal time to stop the polymerization can be further influenced by the reaction temperature. It is expected that the reaction kinetics accelerate with increasing temperature. Information about the ideal polymerization time and temperature was obtained by UV-Vis spectroscopy accompanying the polymerization. Samples were taken from the reaction mixture at certain time intervals, purified and examined with regard to the position of the absorption maximum. Figure 2A shows examples of the UV-Vis spectra (in solution) obtained from the diluted (n-butanol) PEDOT-EthC6 ink after 3 h and after 24 h

(intermediate data points are not shown). The sample is switched to its bright or dark state by chemical oxidation or reduction. A high absorbance modulation is achieved after 3 h polymerization time. The UV-Vis spectra show that after 24 h reaction time the polymerization has proceeded too far. The intensity of the absorption band is reduced, while the position of the absorption band remains at the same wavelength (approx. 630 nm). Although the polymerization continues according to the *in-situ* redox potential measurement and GC/MS analysis, the long-chain polymeric material precipitates and no longer contributes to the color change.

As indicated above, it was found that the best EC properties and thin film quality are obtained at polymerization temperatures of -8°C after 3 h (see Figure 2B, thin film characterization). The polymerization is terminated by solvent extraction (n-heptanol/water). The organic polymer nanoparticles migrate into the organic phase, while the oxidizing agent accumulates in the aqueous phase. The solid content of the purified deep blue polymer dispersion is adjusted for the specific coating requirements by addition of n-butanol.

After addition of n-butanol, the PEDOT-EthC6 ink appears homogeneous. Subsequently, the particle size and zeta potential were determined using dynamic light scattering (DLS) measurements (detailed data can be found in Table S1 and S2). Rather large particle aggregates with an average diameter of 266 ± 20 nm and a polydispersity index (PI) of 0.53 ± 0.17 (particle size) were observed by means of dynamic light scattering analysis. The PI indicates an intermediate state between a monodisperse and a polydisperse polymer suspension, which is due to aggregation and explains the rather large particle diameters.^[26] However, zeta potential measurements showed favorable results with an average value of $+90.5 \pm 10.7$ mV. The large electrostatic repulsion is most likely the reason for the homogeneous appearance of the PEDOT-EthC6 ink. The kinematic viscosity is $7.2 \text{ mm}^2 \text{ s}^{-1}$, making it applicable for R2R slot-die coating and ink-jet printing processes.

In summary, this novel polymerization approach enables wet-chemical coating and printing processes on flexible sub-

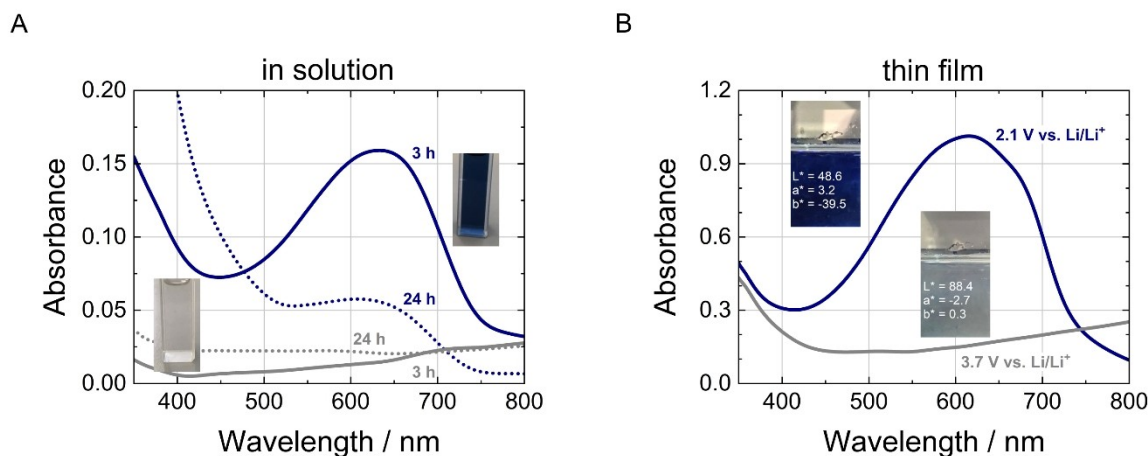


Figure 2. UV-Vis spectra of the diluted (n-butanol) PEDOT-EthC6 ink (chemical oxidation and reduction) as a function of polymerization time after 3 h and after 24 h (A) and *in-situ* spectroelectrochemical data as well as photographic images and $L^*a^*b^*$ color coordinates of the nano-PEDOT-EthC6 thin films (B).

strates to be implemented in a straightforward way, which makes it a simplified and viable alternative to the *in-situ* polymerization of EDOT derivatives and a more flexible method adapted to the needs of ECPs when compared to the established *BAYTRON P* synthesis. The novel preparation method is not limited to water soluble monomers and does not require the use of dispersing agents such as PSS, which is an electro-optically inactive component that compromises the EC performance of the resulting active thin films.

Compared to conventional oxidative polymerization routes in solution, the novel method does not require a complex re-dispersion step and therefore offers advantages in terms of optical film quality.^[10,11] In contrast to R2R *in-situ* polymerization, the dispersion route proposed requires neither a reactive coating step, nor a rinsing step, resulting in an overall process simplification for further cost reduction of ECP thin film production. The deposition is therefore easier to control during coating and is applicable to a variety of wet-chemical deposition methods. Furthermore, the nanoscale ink stands out in terms of atom economy and other green chemistry metrics. In the R2R *in-situ* polymerization process, considerable losses of monomer have to be tolerated during rinsing. In comparison, less monomer is presumably lost in the present dispersion route and recovery is conceivable.^[7]

2.2. Optical and Spectroelectrochemical Characterization

For thin film deposition, the PEDOT-EthC6 ink was spin-coated on flexible PET-ITO substrates at 200 rpm for 30 s and subsequently annealed in a circulating air oven at 100 °C for 90 min. The spectroelectrochemical characterization of the nano-PEDOT-EthC6 thin films on PET-ITO is depicted in Figure 2B. The absorption spectra illustrate that the color neutral bright state (charged) is reached at potentials of 3.7 V vs. Li/Li⁺. The bright state transmittance T_{bright} is 70 % (620 nm). At potentials of 2.1 V vs. Li/Li⁺, a strong and broad absorption with a maximum at approx. 620 nm is responsible for the deep blue

color that occurs when the PEDOT backbone is discharged from its oxidized bipolaron state (bright) to its uncharged state (dark). The dark state transmittance T_{dark} is 10 % (620 nm), resulting in a contrast ratio ($CR = T_{\text{bright}}/T_{\text{dark}}$) of 7.0. The coloration efficiency ($\eta = \log(T_{\text{bright}}/T_{\text{dark}})/q$) at the absorption maximum is calculated to be 245 cm² C⁻¹.

The analysis of the optical properties (CIELAB color space and visible light transmittance τ_v) further confirms the neutral tint of the bright state and the large optical contrast. The color coordinates in the bright state are $L^* = 88.4$, $a^* = -2.7$, $b^* = -0.3$, while the visible light transmittance τ_v is 73 %. The dark state shows a visible light transmittance τ_v of 16 % and the color coordinates are $L^* = 48.6$, $a^* = 3.2$, $b^* = -39.5$. Nano-PEDOT-EthC6 thin films prepared according to the novel route exhibit similar properties in terms of color neutrality, transmissivity in the bright state and optical contrast when compared to the *in-situ* polymerized material.^[7]

In Figure 3, scanning electron microscopy (SEM) images of a nano-PEDOT-EthC6 thin film are depicted. The thin film shows a grainy, but smooth surface. In comparison, the *in-situ* polymerized PEDOT-EthC6 thin films appear as a characteristic three-dimensional, periodical honeycomb pattern (Figure S2). The honeycomb structure is ascribed to the rinsing process of the solid PEDOT-EthC6 thin films, in which the remaining oxidizing agent, residual monomer, short-chain oligomers and other byproduct are removed from the polymer film.^[7] The novel approach does not require any rinsing of the thin films, since the excess oxidizing agent is removed before coating. As can be taken from the SEM images, this leads to significantly less surface roughness, which can also cause light scattering (reflection haze). In addition, the high uniformity is supported by low haze values of the nano-PEDOT-EthC6 thin films of approx. 2 %. Haze comprises all types of light scattering caused by dry particulates, be it from small or larger particles, dispersed in a medium. For the nano-PEDOT-EthC6 thin films, this means that only very little light is scattered at wide angles or diffused due to macroscopic irregularities.

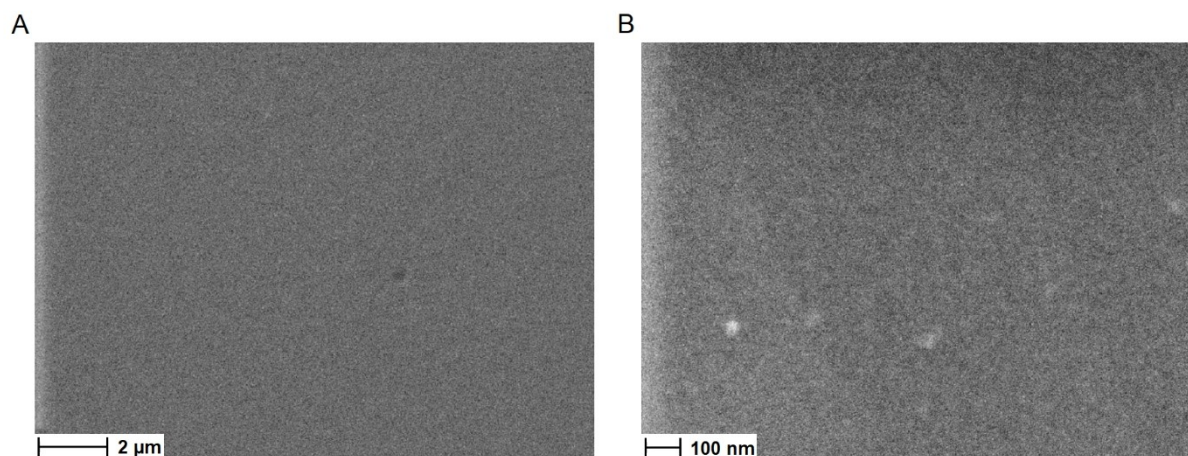


Figure 3. Characteristic SEM images of a nano-PEDOT-EthC6 thin film as an overview image (A) and at higher magnification (B). The thin film shows a grainy, but smooth surface.

2.3. Electrochemical Characterization

The electrochemical properties of the nano-PEDOT-EthC6 thin films were initially investigated by cyclic voltammetry (CV). Figure 4A shows the CVs at a scan rate of 10 mV s^{-1} (red line). The thin films exhibit reversible redox peaks at potentials of 2.7 V (anodic scan) and 3.0 V vs. Li/Li^+ (cathodic scan) corresponding to the oxidation (decoloration) and reduction (coloration) process, respectively, of the conjugated backbone. The substantially broadened cathodic and anodic half-waves are an unavoidable consequence of hindered diffusion and insertion of the counter anions as well as molecular inhomogeneities in the polymer matrix (e.g. different chain length, different sizes of crystalline domains, polymer particle dimensions, and pore dimensions). The in-homogeneities affect the redox potentials, but are not expected to compromise cycling stability. The coulombic efficiency is approx. 1, indicating a reversible redox process. The results from the CV measurements are in agreement with previously published data

of the *in-situ* polymerized PEDOT-EthC6 thin films. These films exhibit also a reversible redox behavior including an anodic process with a peak at approx. 2.8 V vs. Li/Li^+ (anodic scan) and a broad cathodic process with a peak at approx. 2.5 V vs. Li/Li^+ (cathodic scan).^[7] Furthermore, the results from the CV analysis are comparable with previously published data of similar PEDOT and PEDOT-like species.^[5,27]

Figure 4B shows the CVs of nano-PEDOT-EthC6 thin films at various scan rates from 5 to 100 mV s^{-1} . The redox peaks are shifted by approx. 200 mV when scan rates between 5 mV s^{-1} and 100 mV s^{-1} are applied. The small shifts indicate fast reaction kinetics and promise a prompt response in prospective ECDs.

The PEDOT-EthC6 films were further characterized by galvanostatic charging/discharging experiments. First, the redox behavior was investigated as a function of the charging/discharging rate with current densities between $1 \mu\text{A cm}^{-2}$ and $1,000 \mu\text{A cm}^{-2}$ (Figure 5A). The charge and discharge curves show a reversible oxidation and reduction behavior, while the

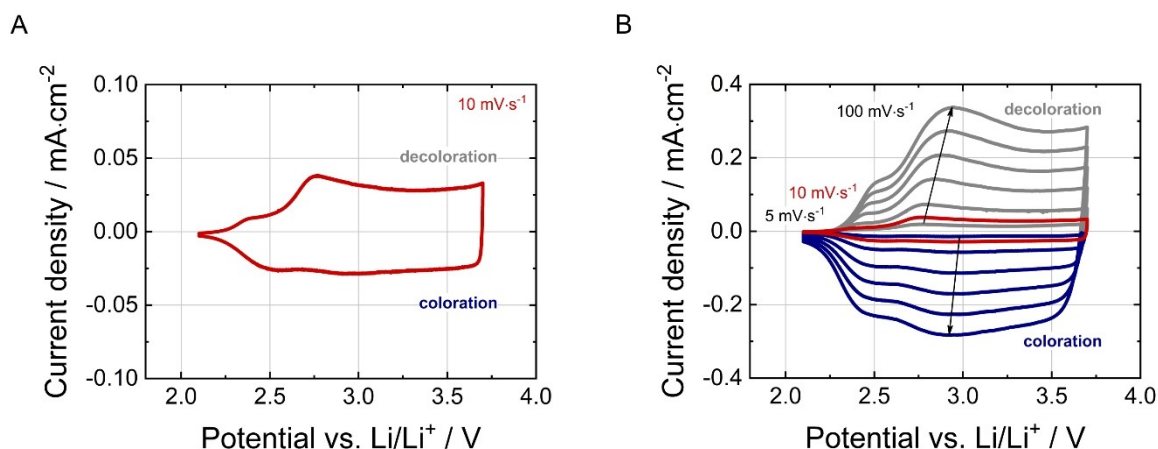


Figure 4. Cyclic voltammograms of the nano-PEDOT-EthC6 thin films (5 cycles) at a scan rate of 10 mV s^{-1} (A) and as a function of the scan rate ranging from 5 mV s^{-1} to 100 mV s^{-1} (B).

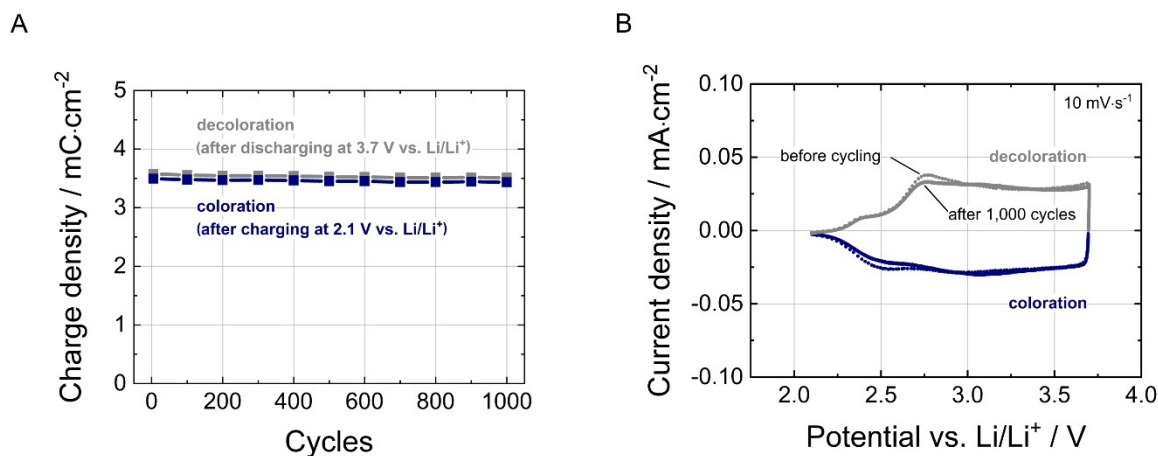


Figure 5. Charge/discharge curves of the nano-PEDOT-EthC6 thin films as a function of current density ranging from $1 \mu\text{A cm}^{-2}$ to $1,000 \mu\text{A cm}^{-2}$ (A) and during cycling at a current density of $50 \mu\text{A cm}^{-2}$ (B).

coulombic efficiency is approx. 1 for all charging/discharging rates. The charge density of the EC thin films is determined after the discharge (reduction) process at 2.1 V vs. Li/Li^+ and depends on the applied current density. The nano-PEDOT-EthC6 film exhibits a maximum charge density of 3.8 mC cm^{-2} at a current density of $1 \mu\text{A cm}^{-2}$. The high current density indicates high film thickness of the EC layers. This enables a high optical contrast and, in particular, a highly absorbing dark state. However, due to the structure of PEDOT-EthC6, the bright state exhibits color neutrality and high transmissivity. As further revealed in Figure 5A, the overpotential increases with the charge and discharge rate (current density). This becomes apparent by a shift of the potential curve to higher values during charging to lower values during discharging.

Second, cycling stability measurements of the PEDOT-EthC6 thin films were performed by means of galvanostatic charging/discharging experiments at a current density of $50 \mu\text{A cm}^{-2}$. The individual charge and discharge curves are shown in Figure 5B. Over the course of 1,000 cycles, there is an almost perfect overlap of the individual curves. The identical shape of the curves along with the unchanged overpotential over the course of 1,000 cycles indicate EC thin films with high cycling stability.

The results from the cycling stability measurements are further evaluated in Figure 6A. The results of the charge density analysis during charging/discharging indicate a highly reversible redox switching behavior (coulombic efficiency above 98%). The charge density, with values of approx. 3.5 mC cm^{-2} after charging/discharging, remains almost constant over the course of 1,000 switching cycles. The total charge retention is higher than 98% after 1,000 cycles. CV measurements before and after the cycling stability measurements are depicted in Figure 6B. The CVs overlap almost perfectly. Small deviations are due to formation processes as well as hindered diffusion and insertion of the bis(trifluoromethanesulfonyl)imide anions (TFSI^-) during the first few cycles.

In summary, nano-PEDOT-EthC6 thin films prepared from the novel PEDOT-EthC6 ink exhibit similar electrochemical behavior to that of the *in-situ* polymerized material. The cycling

stability is remarkable, indicating high purity and stability of the EC thin films. This emphasizes the effective processing steps during the preparation of the PEDOT-EthC6 ink. In particular, the results imply that the coating ink consists solely of polymer (which itself has structural in-homogeneities on the molecular level) and solvents (n-butanol and n-heptanol). Impurities that could affect the cycle stability, e.g. residues of the oxidizing agent, were effectively removed. In this context, the preparation and purification of the PEDOT-EthC6 ink has clear advantages when compared to the complex rinsing process of the *in-situ* polymerized thin films.^[7]

3. Conclusion

A novel polymerization approach has been demonstrated with the EDOT-EthC6 monomer (a sidechain-modified EDOT derivative), combining the advantages of *in-situ* polymerization and standard cross-coupling polymerization followed by re-dispersion. The resultant PEDOT-EthC6 nanoparticles form inks having prolonged shelf life and characteristics compatible with high-throughput coating and printing processes on flexible, conductive substrates. Nano-PEDOT-EthC6 thin films deposited according to the new procedure achieve similar EC properties concerning cycling stability and color neutrality in the bright state when compared to thin films resulting from the previously developed *in-situ* polymerization process. In addition, the new process is advantageous in terms of overall sustainability due to the exclusive use of less toxic solvents and easier process control. These results make both the materials and the polymerization approach attractive for cost-effective ECDs with low environmental impact. Ongoing research is focused on prolonged cycling and durability tests, life cycle assessment considerations as well as the assembly and characterization of proof-of-concept ECDs with suitable ion storage electrodes and electrolytes. In parallel, the implementation of the PEDOT-EthC6 ink in thin film deposition techniques, such as R2R slot-die coating, ink-jet or screen-printing is targeted.

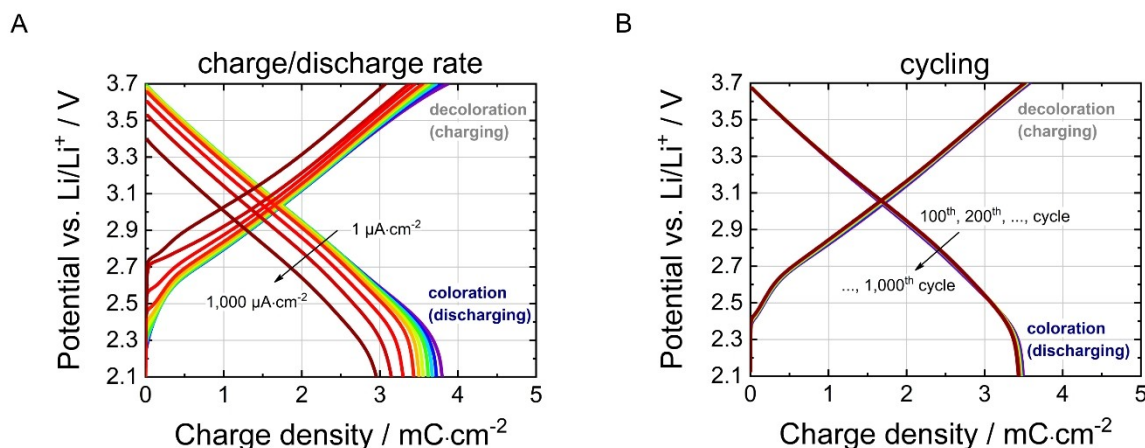


Figure 6. Charge/discharge density (A) of the nano-PEDOT-EthC6 thin films over the course of 1,000 cycles and CV curves (B) collected before (dotted line) and after cycling (solid line).

Experimental Section

Materials: PET-ITO films from Eastman Chemical Company (Flexvue™ OC50, sheet resistance: approx. 50 $\Omega/\text{sq.}$) were used as transparent, conductive substrates. The EDOT-EthC6 monomer was provided by Centrum Organické Chemie s.r.o. (COC), Rybitví, Czech Republic and was used as received. Iron (III)-tosylate, used as oxidizing agent, is commercially available from Hereaus as a 60 w.-% mixture in ethanol (Clevios C-E60). Other reagents were purchased from Sigma Aldrich and were used without further purification.

Preparation of the PEDOT-EthC6 ink: The PEDOT-EthC6 ink was prepared in a double-walled reaction vessel equipped with a mechanical stirrer. Iron (III)-tosylate (2.25 mol) was dissolved in acetonitrile (255 mol) and distilled water (13.5 mol) at 25 °C. EDOT-EthC6 (1 mol) was added under stirring. The resulting polymerization mixture was added to the cooled (-8 °C) doubled-walled reaction vessel and the polymerization was allowed to continue for 3 h. Afterwards, the polymerization was terminated by solvent extraction. For this purpose, the reaction mixture was added into n-heptanol (12 mol) and the solvent extraction was performed in a separatory funnel using distilled water, acidified with 1 M hydrochloric acid (pH 2–3) as the aqueous phase. The solvent extraction was repeated three times. The resultant deep blue polymer ink was filtered via a syringe filter (5 μm). The solid content of the ink was adjusted to the specific coating requirements by addition of n-butanol (for example 24 mol).

Preparation of the nano-PEDOT-EthC6 thin films: Spin coating was performed by means of a KSM Karl-Süss spin coater model RC8. The PEDOT-EthC6 ink was spun off at 200 rpm for 30 s. The resulting thin films were annealed for 90 min at 100 °C in a circulating air oven.

Characterization of the PEDOT-EthC6 ink: In-situ redox potential and conductivity measurements of the polymerization mixture during the polymerization process were performed in a conical 100 mL glass vessel, equipped with a mechanical stirrer. The experiments were executed under argon atmosphere at room temperature with platinum as working and counter electrode and a saturated calomel electrode (SCE) as reference. A potentiostat/galvanostat type VMP3 from Bio-Logic Science Instruments SAS was used. UV-Vis spectra of the PEDOT-EthC6 ink were recorded using a SEC2000 spectrometer (ALS). GC/MS measurements of the PEDOT-EthC6 ink were performed with a gas chromatograph type Clarus 500 from Perkin Elmer, equipped with an auto sampler and a mass spectrometer. Samples were prepared by solvent extraction with n-heptanol and distilled water, oxidized with sodium thiosulfate and diluted with ethanol. Hydrodynamic diameters and zeta potential of the PEDOT-EthC6 nanoparticles were analyzed by dynamic light scattering (DLS, Malvern Instruments Zeta Sizer). Kinematic viscosity of the PEDOT-EthC6 ink was measured with a Schott AVS 400 capillary viscometer.

Characterization of the nano-PEDOT-EthC6 thin films: In-situ spectroelectrochemical, UV-Vis and colorimetric measurements (CIELAB color space) of the spin-coated nano-PEDOT-EthC6 thin films deposited from the PEDOT-EthC6 ink on PET-ITO were performed using an Avantes AvaSpec-2048 standard fiber optic spectrometer combined with a balanced deuterium-halogen light source. All (spectro-)electrochemical measurements were executed under argon atmosphere at room temperature with lithium as counter and reference electrode in 1 M LiTFSI/PC liquid electrolyte. A Solartron Multistat 1470E multi-channel potentiostat/galvanostat was used for the electrochemical characterization (cyclic voltammetry, charging/discharging and cycling stability experiments) of the nano-PEDOT-EthC6 thin films deposited from the PEDOT-EthC6 coating dispersion on PET-ITO. The cyclic voltammograms were

recorded with scan rates ranging from 5 to 100 mV s^{-1} . Galvanostatic charge/discharge experiments were performed with current densities ranging from 1 to 1,000 $\mu\text{A cm}^{-2}$. The cycling stability was measured using a galvanostatic charge/discharge procedure for up to 1,000 switching cycles (current density: 50 $\mu\text{A cm}^{-2}$).

Acknowledgements

This work was supported by the European Union's Seventh Framework Program (FP7) and the Horizon 2020 Research and Innovation Program under Grant Agreements nos. 604204 (EELICON) and 760973 (DecoChrom). The authors would like to express their deep gratitude to COC Ltd. (Centrum Organické Chemie s.r.o., Rybitví), Czech Republic, for the supply of the precursor compounds used in this study. The authors further thank César Laia and Thiago Moreira from FCT NOVA - NOVA School of Science and Technology, Lisbon, Portugal, for the DLS measurements referred to in this study. Open access funding enabled and organized by Projekt DEAL.

Conflict of Interest

The authors declare no conflict of interest.

Keywords: electrochromism · electrochromic polymer · PEDOT · neutral-colored bright state · spectroelectrochemistry

- [1] a) S. D. Rezaei, S. Shannigrahi, S. Ramakrishna, *Sol. Energy Mater. Sol. Cells* **2017**, 159, 26–51; b) R. Baetens, B. P. Jelle, A. Gustavsen, *Sol. Energy Mater. Sol. Cells* **2010**, 94, 87–105; c) W. J. Hee, M. A. Alghoul, B. Bakhtyar, O. Elayeb, M. A. Shameri, M. S. Alrubaih, K. Sopian, *Renewable Sustainable Energy Rev.* **2015**, 42, 323–343; d) C. M. Lampert in *Large-Area Chromogenics: Materials and Devices for Transmittance Control*, Vol. 10304 (Eds.: C. M. Lampert, C.-G. Granqvist), SPIE Proceedings, Bellingham, USA, **2017**, pp. 1–18; e) C. G. Granqvist, E. Avendaño, A. Azens, *Thin Solid Films* **2003**, 442, 201–211; f) C. G. Granqvist, P. I. Bayrak, G. A. Niklasson, *Surf. Coat. Technol.* **2018**, 336, 133–138.
- [2] a) C. G. Granqvist, *Electrochim. Acta* **1999**, 44, 3005–3015; b) D. Rosseinsky, R. J. Mortimer, *Adv. Mater.* **2001**, 13, 782–793; c) C. M. Lampert, *Mater. Today* **2004**, 7, 28–35.
- [3] L. B. Groenendaal, F. Jonas, D. Freitag, *Adv. Mater.* **2000**, 12, 481–494.
- [4] a) H. W. Heuer, R. Wehrmann, S. Kirchmeyer, *Adv. Funct. Mater.* **2002**, 12, 89–94; b) W. T. Neo, Q. Ye, S.-J. Chua, J. Xu, *J. Mater. Chem. C* **2016**, 4, 7364–7376.
- [5] L. Groenendaal, G. Zotti, P.-H. Aubert, S. M. Waybright, J. R. Reynolds, *Adv. Mater.* **2003**, 15, 855–879.
- [6] C. J. Du Bois, F. Larmat, D. J. Irvin, J. R. Reynolds, *Synth. Met.* **2001**, 119, 321–322.
- [7] S. Macher, M. Schott, M. Sassi, I. Facchinetti, R. Ruffo, G. Patriarca, L. Beverina, U. Posset, G. A. Giffin, P. Löbmann, *Adv. Funct. Mater.* **2020**, 30, 1906254.
- [8] a) P. M. Beaujuge, S. Ellinger, J. R. Reynolds, *Nat. Mater.* **2008**, 7, 795–799; b) A. M. Österholm, D. E. Shen, D. S. Gottfried, J. R. Reynolds, *Adv. Mater.* **2016**, 1, 1600063; c) L. Beverina, G. A. Pagani, M. Sassi, *Chem. Commun.* **2014**, 50, 5413–5430; d) C. M. Amb, A. L. Dyer, J. R. Reynolds, *Chem. Mater.* **2011**, 23, 397–415; e) S. Ellinger, K. R. Graham, P. Shi, R. T. Farley, T. T. Steckler, R. N. Brookins, P. Taranekar, J. Mei, L. A. Padilha, T. R. Ensley, et al., *Chem. Mater.* **2011**, 23, 3805–3817.
- [9] P. M. Beaujuge, J. R. Reynolds, *Chem. Rev.* **2010**, 110, 268–320.
- [10] A. M. Österholm, D. E. Shen, J. A. Kersulis, R. H. Bulloch, M. Kuepfert, A. L. Dyer, J. R. Reynolds, *ACS Appl. Mater. Interfaces* **2015**, 7, 1413–1421.

- [11] J. A. Kerszulis, K. E. Johnson, M. Kuepfert, D. Khoshabo, A. L. Dyer, J. R. Reynolds, *J. Phys. Chem. B* **2015**, *3*, 3211–3218.
- [12] M. Sassi, M. M. Salamone, R. Ruffo, G. E. Patriarca, C. M. Mari, G. A. Pagani, U. Posset, L. Beverina, *Adv. Funct. Mater.* **2016**, *26*, 5240–5246.
- [13] S. Macher, M. Schott, M. Dontigny, A. Guerfi, K. Zaghib, U. Posset, P. Löbmann, *Adv. Mater.* **2020**, 2000836.
- [14] a) J. Jensen, F. C. Krebs, *Adv. Mater.* **2014**, *26*, 1–4; b) J. Jensen, M. Hösel, A. L. Dyer, F. C. Krebs, *Adv. Funct. Mater.* **2015**, *25*, 2073–2090.
- [15] a) B. D. Reeves, C. R. G. Grenier, A. A. Argun, A. Cirpan, T. D. McCarley, J. R. Reynolds, *Macromol.* **2004**, *37*, 7559–7569; b) G. S. Collier, I. Pelse, J. R. Reynolds, *ACS Macro Lett.* **2018**, *7*, 1208–1214.
- [16] C. L. Gaupp, D. M. Welsh, R. D. Rauh, J. R. Reynolds, *Chem. Mater.* **2002**, *14*, 3964–3970.
- [17] C. L. Gaupp, D. M. Welsh, J. R. Reynolds, *Macromol. Rapid Commun.* **2002**, *23*, 885–889.
- [18] R. M. Walczak, J. S. Cowart, J. R. Reynolds, *J. Mater. Chem.* **2007**, *17*, 254–260.
- [19] M. Sassi, M. M. Salamone, R. Ruffo, C. M. Mari, G. A. Pagani, L. Beverina, *Adv. Mater.* **2012**, *24*, 2004–2008.
- [20] A. Cochet, PhD thesis, Julius-Maximilians-Universität, Würzburg, Germany, **2008**.
- [21] a) A. Kumar, D. M. Welsh, M. C. Morvant, F. Piroux, K. A. Abboud, J. R. Reynolds, *Chem. Mater.* **1998**, *10*, 896–902; b) G. Gunbas, L. Toppare, *Chem. Commun.* **2012**, *48*, 1083–1101; c) S. Miyaniishi, K. Tajima, K. Hashimoto, *Macromol.* **2009**, *42*, 1610–1618; d) D. Bagnis, L. Beverina, H. Huang, F. Silvestri, Y. Yao, H. Yan, G. A. Pagani, T. J. Marks, A. Facchetti, *J. Am. Chem. Soc.* **2010**, *132*, 4074–4075.
- [22] S. Kirchmeyer, K. Reuter, *J. Mater. Chem.* **2005**, *15*, 2077–2088.
- [23] T. Johansson, L. A. A. Pettersson, O. Inganäs, *Synth. Met.* **2002**, *129*, 269–274.
- [24] S. Garreau, G. Louam, S. Lefrant, J. P. Buisson, G. Froyer, *Synth. Met.* **1999**, *101*, 312–313.
- [25] a) K. E. Aasmundtveit, E. J. Samuelsen, L. A. A. Pettersson, O. Inganäs, T. Johansson, R. Feidenhans'l, *Synth. Met.* **1999**, *101*, 561–564; b) L. A. A. Pettersson, T. Johansson, F. Carlsson, H. Arwin, O. Inganäs, *Synth. Met.* **1999**, *101*, 198–199; c) D. M. de Leeuw, E. J. Lous, *Synth. Met.* **1994**, *65*, 45–53.
- [26] C. A. T. Laia, P. López-Cornejo, S. M. B. Costa, J. d'Oliveira, J. M. G. Martinho, *Langmuir* **1998**, *14*, 3531–3537.
- [27] S. Dulaud, B. Ouvrard, A. Celik-Cochet, G. Campet, U. Posset, G. Schottner, M.-H. Delville, *J. Phys. Chem. B* **2010**, *114*, 7445–7451.

Manuscript received: December 22, 2020

Revised manuscript received: January 19, 2021

Accepted manuscript online: February 3, 2021